Visualization of internal damage in RC slab with single side access attenuation tomography

Clément Granier[1)], Tomoki Shiotani[2)], Katsufumi Hashimoto [2)] and Takahiro Nishida [2)]
1) School of Architecture, civil and environmental engineering, École Polytechnique Fédérale de Lausanne, Route cantonale, 1015 Lausanne, Switzerland.
2) Graduate school of Engineering, Kyoto University, C3-b4S14, Kyoto-Daigaku-Katsura, Nishikyo-ku, Kyoto 615-8540, Japan.

ABSTRACT: An innovative non-destructive testing method is developed and introduced for inspecting the interior of concrete. The method is based on the phenomenon of attenuation, which corresponds to the gradual loss in amplitudes of waves traveling through a heterogeneous medium. In the case of concrete, the attenuation is particularly high in the presence of defects, such as cracks or air voids. Ingeniously, single-side measurements of acoustic emission (AE) activity are employed for reconstructing distribution of the wave attenuation rate in the tested concrete and thus locating damaged areas. The present method is successfully applied to a panel of a reinforced concrete slab of a bridge in service.

1 INTRODUCTION

Acoustic emission (AE) testing is one of non-destructive testing (NDE) methods available for investigating the internal features of civil engineering structures. AE techniques have been extensively used for bridge examination [1-3]. AE phenomena correspond to the release of internal energy in the form of elastic waves when cracks are nucleated and extend (referred to as primary AE activity) or internal fretting on cracked surfaces (referred to as secondary AE activity) [4]. A sensing system for recording AE activity has been already published [5]. Sources of AE events, namely cracks, are located from the measured arrival times of their associated waves [6, 7]. Their cracking modes can be determined through the moment tensor analysis [8, 9].

Nowadays, AE source location is ingeniously combined with a travel-time tomography to reconstruct the wave velocity distribution inside concrete [10]. Indeed, the decrease in the wave velocity substantially corresponds to the presence of such defects as cracks or air voids [11].

Amplitudes of elastic waves tend to decrease while they are traveling through media such as concrete. This phenomenon is well known as an attenuation, resulting from heterogeneous nature of concrete and from wave characteristics of diffraction, dispersion and scattering at the boundaries in addition to geometrical spreading [12]. The presence of defects in concrete, such as cracks or air voids, could enhance the attenuation [13]. It has been shown that the attenuation was more sensitive to the presence of defects than the velocity distribution [14]. H.K. Chai et al. [15] employed the attenuation of ultrasounds for imaging the interior of concrete. Their method has been proven to be effective for locating damages in concrete. However, it has one disadvantage to require an access to at least two sides of the tested specimen. In the case of bridge slabs, it is generally not possible to measure at the two sides because of traffic. Accordingly surface waves have been employed to investigate the interior damage of concrete [16] ; however, specific depths could not so far be identified with this technique.

In the present paper, an innovative method is developed for reconstructing distribution of the attenuation rate inside a reinforced concrete element from single-side measurements of AE activity. Applied results of this method to a panel of a reinforced concrete (RC) bridge slab is discussed.

2 ALGORITHM FOR ATTENUATION TOMOGRAHY

2.1 *General principle*

The attenuation rate in a particular medium can be defined as the amplitude decay undergone by an elastic wave traveling in this medium, per unit of distance. It is generally expressed in decibels per meter (dB/m). The increase in the attenuation rate generally indicates the presence of defects in concrete, such as cracks or air voids.

For computing the attenuation tomography, the method combines a conventional AE source location algorithm with an algorithm of tomographic reconstruction, known as a SIRT algorithm (Simultaneous Iterative Reconstruction Technique).

The process is summarized in Figure 1. It is noted that AE activity can be measured from only one side of the tested member. First, the source locations of all AE events are used as input, where a constant wave velocity across the tested member is assumed for calculation. Second, the amplitude at the source of the considered AE event is

estimated on the basis of the amplitudes recorded by the sensors. Third, the attenuation rates along all the wave paths between the source and the receiving sensors are computed.

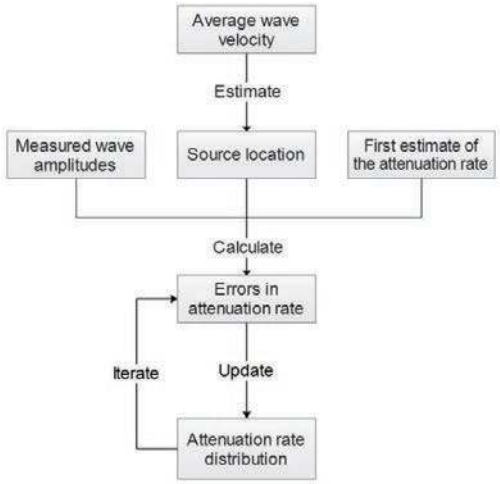

Figure 1: Flow chart to compute attenuation tomography

2.2 *Source location algorithm*

The algorithm for AE source location is based on the Inglada's method, which is used in seismic engineering for locating the epicenter of earthquakes [6, 7]. By assuming a constant wave velocity inside the tested specimen, the source location of an AE event is determined from the arrival times of their associated elastic waves at the locations of several sensors.

2.3 *Estimation of the peak amplitude at the source*

For each AE event, the peak amplitude of the elastic wave at the source is unknown. Consequently, it must be approximated to calculate the attenuation rate along the considered wave paths. In the tomography algorithm, the attenuation rate is generally estimated from a relation represented in Figure 2. First, the peak amplitude of the signal recorded by each sensor is plotted as a function of the distance between the source and the sensors. Second, a linear regression between the peak amplitude of the elastic wave and the distance from the source is computed. The peak amplitude at the source is referred to as equal to the value for the case that the distance is equal to zero.

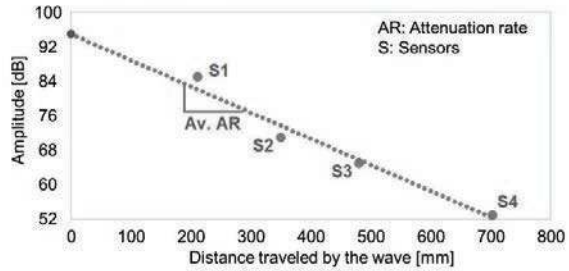

Figure 2: Estimation of the peak amplitude of the elastic wave at the source

2.4 *SIRT algorithm for attenuation tomography*

In the tomography based on the attenuation, the area of interest and analyzed must be divided into mesh elements characterized by their own attenuation rates. Then, a first estimate on distribution of the attenuation rates is to be provided as input. By comparing the measured attenuation rate along each wave path to its calculated value of the assumed distribution, the SIRT algorithm could lead to proper distribution of the attenuation rates.

First, the measured attenuation rate along each ray path is estimated from Equation 1.

$$AR_{measured,i} = \frac{A_{source} - A_{sensor,i}}{\sum_j^{N_i} d_{i,j}} \quad (1)$$

Where:
$AR_{measured,i}$: measured average attenuation rate along the wave path from the source to the i^{th} sensor
A_{source}: estimated peak amplitude of the elastic wave associated to the considered AE event at its source
$A_{receiver,i}$: peak amplitude of the elastic wave measured at the i^{th} sensor
N_i: mesh number of elements crossed by the wave path from the source to the i^{th} sensor
$d_{i,j}$: length of the wave path from the source to the i^{th} sensor in the j^{th} element

Second, the attenuation rate along each wave path based on distribution of the attenuation rates in the mesh elements is computed by Equation 2.

$$AR_{calculated,i} = \frac{\sum_j^M AR_j \cdot d_{i,j}}{\sum_j^M d_{i,j}} \quad (2)$$

Where:
$AR_{calculated,i}$: calculated average attenuation rate along the wave path from the source to the i^{th} sensor (dB/m)
AR_j: attenuation rate in the j^{th} element (dB/m)
M: mesh number of elements crossed by the ray path from the source to the i^{th} sensor
Afterwards, the difference between the measured and the calculated attenuation rates is calculated for each wave path by using Equation 3.

$$\Delta AR_i = AR_{measured,i} - AR_{estimated,i} \quad (3)$$

In a similar manner to Equation 11, the differences of the attenuation rates on all the wave paths are estimated by Equation 4.

$$\Delta AR_j = \frac{\sum_{i=1}^N \Delta AR_i \cdot d_{i,j}}{\sum_{i=1}^N d_{i,j}} \quad (4)$$

Where N is the number of wave paths crossing the jth element. The attenuation rate in each element is then updated with Equation 5.

$$AR_{j,updated} = AR_j + \Delta AR_j \quad (5)$$

The procedure from Equation 2 through Equation 5 is repeated until the convergence is reached.

3 EXPERIMENT AND MEASUREMENT PROCEDURE

3.1 *Sensor array*

Figure 3 shows the plan view of the bridge and the location of the investigated panel. The panel of dimensions 3750 mm x 2650 mm x 235 mm was tested. The bottom surface of the slab segment is given in Figure 6. As seen, a few cracks are observed. Therefore, it was estimated that the panel (slab segment) was not severely deteriorated according to the visual inspection.
Fifteen AE sensors were placed on the bottom surface of the panel. Figure 7 shows their arrangement. The resonant frequency of AE sensors employed were 30 kHz. The signals detected were amplified by 40 dB by sensor-integrated preamplifier and the signals exceed the threshold of 53 dB were recorded. AE activity under normal traffic loads was monitored for seven days, resulting in total AE events of 53,800,520. The wave velocity for AE source location was initially set at 3300 m/s, which was the average of experimentally measured values at the investigated panel.

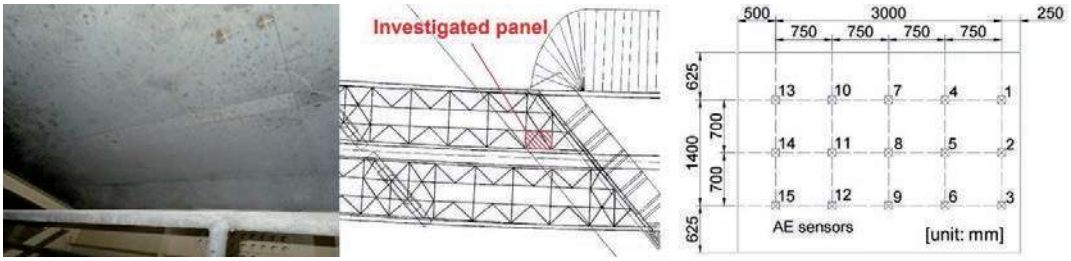

Figure 3: Location overview of the investigated panel and sensor array

3.2 *Panel removal and core sampling*

RC slabs studied herein were fully replaced in November 2015 as other panels in the vicinity of the tested one were so deteriorated as to be replaced. In the course of renovation process, they were cut into parallelepiped pieces. The slab segment corresponding to the investigated panel was preserved for further investigation.

4 RESULTS AND DISCUSSION

The attenuation rate distribution in the investigated panel were computed within the area covered by the sensor array. Parallelepiped-shaped elements of dimensions 375 mm x 350 mm x 60 mm are applied for the meshes. Results are presented in Figure 4 in comparison with the core samples.

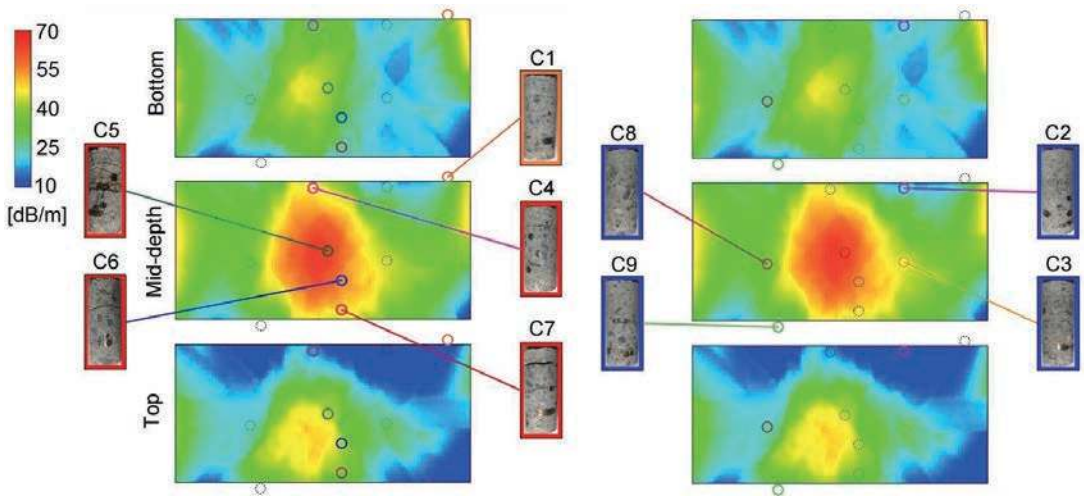

Figure 4: Comparison between the attenuation rate distribution computed and the core samples.

It can be observed that the attenuation rate at the center of the panel is the highest. It suggests that the central part of the panel suffers larger and/or denser cracks than other areas. Furthermore, it appears that the attenuation rates are higher than 40 dB/m at the area, where the core samples have large horizontal cracks (C4, C5, C6 and C7). In contrast, the attenuation rates are lower than 40 dB/m at the area, where the uncracked core samples (C2, C3, C8 and C9) are taken out. These results show that single-side attenuation tomography can be applied to identify severely cracked portions and areas in RC slabs of the bridge in service.

5 SUMMARY

In this paper, an innovative non-destructive method for inspecting the interior of concrete is introduced and applied to the RC slab of a bridge in service. The method, referred to as single-side attenuation tomography, which is based on the principle that the elastic waves traveling through concrete are to impinge on the cracks. It could provide the tomogram on the attenuation rates inside the tested specimen.

To summarize, single-side attenuation tomography must be understood as a very practical non-destructive testing method for identifying the parts of a reinforced concrete member which are very likely to present serious damages. If the tomograms cannot be used, in the present state, for directly assessing the structural safety of the tested specimen, they provide essential information for guiding further investigation.

ACKNOWLEDGEMENTS

A part of this study is commissioned and supported by New Energy and Industrial Technology Development Organization (NEDO). And, we would like express our sincere appreciation and deep gratitude to Dr. Masayasu Ohtsu, Professor Emeritus of Kyoto University, for his prominent suggestions in interpreting the significance of the results of this study.

REFERENCES

[1] T. Shiotani et al., (2012) “Damage evaluation for concrete bridge deck by means of stress wave techniques,” Journal of Bridge Engineering, ASCE, Vol. 17, pp 847-856.

[2] L. Golaski et al., (2002) “Diagnostics of reinforced concrete bridges by acoustic emission,” Journal of Acoustic Emission, Vol, 20, pp 83-98.

[3] T. Shiotani et al., (2007) “Global monitoring of concrete bridge using acoustic emission,” Journal of Acoustic Emission, Vol. 25, pp 308-315.
[4] A. Behnia et al., (2014) “Advanced structural health monitoring of concrete structures with the aid of acoustic emission,” Construction and Building Materials, No. 65, pp 282-302.
[5] M. Ohtsu, (2008) “Acoustic Emission Testing: Basics for Research -Applications in Civil Engineering”, pp 19-40.
[6] V. Salinas et al., (2010) “Localization algorithm for acoustic emission,” Physics Procedia, Vol. 3, pp 863-871.
[7] M. Ge, (2003) “Analysis of source location algorithms”, Journal of Acoustic Emission, Vol. 21, pp 14-28.
[8] M. Ohtsu, (2007) “Acoustic emission techniques standardized for concrete structures,” Journal of Acoustic Emission, Vol. 25, pp 21-32.
[9] M. Ohtsu, (1995) “Acoustic emission theory for moment tensor analysis,” Research in Non-Destructive Evaluation, No. 6, pp 169-184.
[10] F. Schubert, (2004) “Basic principles of acoustic emission tomography,” Journal of Acoustic Emission, Vol. 22, pp 147-158.
[11] A. Behnia et al., (2014) “Integrated non-destructive assessment of concrete structures under flexure by acoustic emission and travel time tomography,” Construction and Building Materials, Vol. 67, pp 202-215.
[12] M. Berthelot et al., (1993) “Study of wave attenuation in concrete,” Journal of Materials Research, Vol. 8, pp 2344-2353.
[13] T.P. Philippidis and D.G. Aggelis, (2005) “Experimental study of wave dispersion and attenuation in concrete,” Ultrasonics, Vol. 43, pp 584-595.
[14] D.G. Aggelis and T. Shiotani, (2008) “Effect of inhomogeneity parameters on wave propagation in cementitious materials,” ACI Materials Journal, pp 187-193.
[15] H.K. Chai et al., (2011) “Tomographic reconstruction for concrete using attenuation of ultrasound,” NDT&E International, Vol. 44, pp 206-2015.
[16] H.K. Chai et al., (2010) Single-side access tomography for evaluating interior defect of concrete, Construction and Buildings Materials 24, 2411-2418.